#519

Contribution to the Twentieth International Conference in High Energy Physics at Madison, Wisconsin, July 17-23, 1980.

Sess. C9 by H. Yuta 7/19/80

INCLUSIVE VECTOR MESON PRODUCTION IN $\nu_\mu D$ CHARGED CURRENT INTERACTIONS

CONF-800724--53

C.C. Chang, W.A. Mann, A. Napier, J. Schneps
Tufts University, Medford, Massachusetts 02155

R.A. Burnstein, J. Hanlon, H.A. Rubin
Illinois Institute of Technology, Chicago, Illinois 60616

C.Y. Chang, T. Dombeck, G.A. Snow, D. Son, P.H. Steinberg
University of Maryland, College Park, Maryland 20742

R. Engelmann, T. Kafka, S. Sommars
State University of New York at Stony Brook, Stony Brook, New York 11974

T. Kitagaki, S. Tanaka, H. Yuta, K. Abe, K. Hasegawa,
A. Yamaguchi, K. Tamai, T. Hayashino, S. Kunori, Y. Ohtani, H. Hayano
Tohoku University, Sendai 980, Japan

MASTER

From hadronic systems induced in 3571 charged-current neutrino-deuterium interactions in the FNAL 15-foot diameter bubble chamber, invariant mass distributions $(\pi^+\pi^-)$ and $(K^\circ_s\pi^\pm)$ have been used to study inclusive production of vector meson resonances. Inclusive rates from a pure iso-scalar target are determined to be 0.05 ± 0.01 $K^{*+}(890)$ per charged-current event and 0.19 ± 0.04 ρ° per charged-current event. Inclusive $K^*(890)^\pm$ production is found to be predominantly $K^{*+}(890)$ in the current fragmentation region. The ratios (ρ°/event) from neutron targets and from proton targets separately are, respectively, 0.18 ± 0.06 and 0.21 ± 0.08. For deuteron targets, trends in the dependence of (ρ°/event) on variables Y_R, W, p_T, and Q^2 are found to be similar to those observed in ρ° production from $\bar{\nu}_\mu p$ collisions.

DE-AC02-76ER03023

I. INTRODUCTION

During the past few years, investigations of inclusive hadron-hadron interactions have indicated that sizeable portions of pion and kaon production originate from the production of well-known resonances, with significant contributions ascribed to the decays of vector mesons ρ°, ω°, and $K^*(890)$.[1-6,9] In hadronically-induced ρ° production, the cross section ratios ρ°/event and ρ°/π^- are characterized by values ~ 0.21 and ~ 0.11, respectively, in $\pi^\pm p$, pp, and non-annihilation $\bar{p}p$ reactions extending from 15 GeV/c to 405 GeV/c incident momentum. Recently, similar ratios of rates have been reported for inclusive ρ° production in hadronic systems excited via charged current neutrino and anti-neutrino interactions. In high energy $\bar{\nu}p$ reactions,[7] for which the hadronic masses W which are excited extend over a range of values with $\langle W \rangle = 3.4$ GeV,

$$\rho^\circ/\text{CC event} = 0.21 \pm 0.03,$$

and

$$\rho^\circ/\pi^- = 0.12 \pm 0.12.$$

In $\nu_\mu p$ reactions having $\langle W \rangle \sim 5$ GeV,

$$\rho^\circ/\text{CC event} = 0.21 \pm 0.04.$$

The similarity of the various ρ° rates suggests "a certain universality of hadronic production",[7] and - in the absence of detailed theory - it is tempting to regard hadron-hadron final states as providing a guide to behavior likely to characterize hadronic systems produced in lepton-nucleon reactions.

Hadronic systems induced by deep-inelastic charged current νN and $\bar{\nu}N$ scattering are at present receiving extensive study, since perturbative Quantum Chromodynamics presumably can be used to predict their non-scaling behavior. In particular, a rise in mean square transverse momentum of the hadronic system with increasing W^2 and Q^2 is expected, as is jet behavior in the variables sphericity, thrust, and energy flow. On the other hand, in πp and pp collisions the inclusively-produced non-strange mesons ($\eta°$, ω, $\rho°$, $f°$) are observed to have production p_T^2 distributions which are exponential and have slope parameter $b \sim 3.4$ $(GeV/c)^{-2}$;[2] these distributions are broader in p_T^2 than those which characterize $\pi^{\pm}$ mesons for which b is typically ~ 9 $(GeV/c)^{-2}$. Similarly, p_T^2 distributions for inclusive $K^*(890)$ are observed to be broader than those for $K_s^°$ production.[9] Thus, it is possible that p_T^2-broadening of hadronic systems with increasing excitation energy or four-momentum transfer may, in part, reflect changes in relative contributions from higher mass resonances, rather than the onset of QCD processes. It is likely that comparisons of QCD calculations with neutrino data can be rendered more meaningful if the contributions of resonances to behavior of $\nu/\bar{\nu}$-induced hadronic systems is delineated. To this end, We report a new study of the inclusive reactions

$$\nu_\mu + D \rightarrow \mu^- + K^{*\pm}(890) + \text{anything} \qquad (1)$$
$$\hookrightarrow K_s^° \pi^{\pm}$$

and

$$\nu_\mu + D \rightarrow \mu^- + \rho° + \text{anything} \qquad (2)$$
$$\hookrightarrow \pi^+\pi^-.$$

II. EVENT SELECTION

Neutrino interactions were recorded in a 328,000 picture exposure of the Fermilab 15-foot diameter, deuterium-filled bubble chamber exposed to a wide-band, single horn focussed neutrino beam during the period November 1978 until January 1979. The neutrino beam was produced using a primary beam of 350 GeV/c protons incident upon a beryllium oxide target, with a total flux of 4.9×10^{18} incident protons. For the present analysis, charged current reactions (1) containing visible K_s° were taken from about 85% of the exposure, while charged-current events without visible signs of strangeness were obtained from about one-third of the film. Charged current candidates are selected according to a kinematic method, which used the following criteria:

1) An event must have a candidate μ^- track, i.e. a track having largest negatively-charged transverse momentum component perpendicular to the beam (p_T^-), which does not interact within the visible fiducial volume, and whose momentum component transverse to the remaining visible hadrons is $p_{TR} > 1$ GeV/c.

2) The event's interaction vertex must occur inside a fiducial volume of 15.6 m^3 (corresponding to $\simeq$ 2.4 tons of deuterium).

3) The event's total visible energy must be greater than 5 GeV.

4) The incident neutrino's energy is estimated using the method of H.G. Heilmann, namely

$$E_\nu = p_\ell^{\mu^-} + p_\ell^c + p_\ell^c * \frac{|\vec{p}_t^{\mu^-} + \vec{p}_t^c|}{p_t^c} .$$ We require $E_\nu > 10$ GeV.

5) The candidate μ^-'s LAB momentum is required to be > 2 GeV/c.

A total of 3571 events satisfied these criteria and constituted our charged current sample for analysis. By imposing identical cuts on samples of charged current events simulated using the Monte Carlo technique, the fraction of real charged current interactions with E > 10 GeV removed by our procedures is estimated to be $\sim$ 16%. This loss results primarily from the restriction p_{TR} > 1 GeV on muon tracks which however is needed in order to minimize contamination from neutral current reactions, and also from $\bar{\nu}N$ and neutral hadron-induced backgrounds. It is assumed in the following that the above selections remove charged current events in a manner uncorrelated with resonance production.

III. $K^*(890)$ PRODUCTION

For high energy charged-current neutrino-nucleon interactions, the quark-parton model together with the assumption that flavor-changing valence quark processes dominate, provide a particularly simple framework for discussion. In $\nu(\bar{\nu})$ + nucleon collisions, the $W^+(W^-)$ vector boson strikes a valence d (u) quark changing it into a "fast" u (d) quark. In experiments using liquid deuterium fills, the target nucleons are nearly free neutrons or protons consisting of (ddu) or (uud) valence quarks. To consider inclusive $K^*(890)$ production from our neutrino-deuterium interactions, we note that $K^{*+} = u\bar{s}$ and hence can receive a struck valence quark whereas $K^{*-} = \bar{u}s$ does not have this advantage. We thus expect that $\sigma_{CC}(K^{*+}) > \sigma_{CC}(K^{*-})$ in our data, and additionally that the produced $K^{*+}(890)$ will be predominantly current fragments.

Our charged current sample contained 180 events which are of the type reaction (1); their $K^\circ_s\pi^\pm$ invariant mass combinations are displayed in Fig. 1. A signal of $\sim(40 \pm 5)$ $K^{*\pm}(890)$ combinations is evident in the plot. The dots represent a combinatorial background estimate, whose shape was obtained by pairing K°_s's together with π^+ or π^- from different events which had the same charge multiplicity and similar hadronic masses, and whose amount was determined by overall normalization. The shaded regions in the plot show the $K^\circ_s\pi^+$ combinations only. In the $K^{*+}(890)$ region we observe $\sim(37 \pm 5)$ K^{*+} combinations above the combinatorial background, from which we conclude that most of the $K^{*\pm}(890)$ signal is indeed $K^{*+}(890)$. Using the combinatorial background, we find

$$\frac{(K^{*+})_{CC}}{\text{Charged Current Event}} = 0.05 \pm 0.01,$$

$$\frac{(K^{*+})_{CC}}{(K^\circ_s)_{CC}} = 0.23 \pm 0.03;$$

where the errors quoted represent statistical errors only.

In studies of inclusive $\pi^\pm$ production from high energy $\nu/\bar{\nu}\cdot p$ reactions, a produced hadron's center-of-mass rapidity Y_R is found to be effective in separating target from current fragments.[10] In Figs. 2(a) and 2(b), we show the invariant masses of $K^\circ_s\pi^+$ combinations separated according to whether a combination's rapidity occurs in the forward or backward CM hemisphere. *No K^{*+} signal is discernable among combinations* having $Y_R < 0.0$. Essentially all of the $K^{*+}(890)$ signal in our data occurs in the forward CM region, indicating that the bulk of $K^{*+}(890)$ production in charged-current neutrino reactions results from current fragmentation processes.

IV. ρ° PRODUCTION

In the Quark parton model the ρ° and ω vector mesons contain equal mixtures of u and d quarks:

$$\rho^\circ = \frac{1}{\sqrt{2}}\,(u\bar{u} - d\bar{d}), \qquad \omega^\circ = \frac{1}{\sqrt{2}}\,(u\bar{u} + d\bar{d}).$$

Under the assumption that valence quark processes dominate inclusive vector meson production, one expects that integrated or differential inclusive rates expressed as ratios, i.e.

$$\frac{d\sigma\ (\nu/\bar{\nu} + N \rightarrow \mu^{\mp} + \rho^\circ(\omega^\circ) + \text{anything})}{\sigma_{\nu/\bar{\nu}}\ (\text{Charged current events})} \qquad (3)$$

to be similar for $\nu_\mu N$ and $\bar{\nu}_\mu N$ reactions. This expectation is born out by the near-equality of the overall inclusive rates ρ°/event reported recently from analysis of high energy $\bar{\nu}p$ and νp data.[7,8] In the $\bar{\nu}p$ experiment, differential rates for inclusive ρ° production in the variables Y_R, W, Q^2, p_T, and z are reported;[7] in the νp analysis a different background prescription in the $\rho^\circ \rightarrow \pi^+\pi^-$ invariant mass region is used, and only the multiplicity-dependence of ρ° production is extracted. In this experiment we have measured ρ° production overall inclusively from deuteron, neutron, and proton targets. It should be emphasized that since the ρ° is a broad resonance ($\Gamma \simeq 150$ MeV), the separation of ρ° signals from non-resonant background or from structure related to other resonances is not particularly straightforward. In the following, we summarize results obtained by using two different background methods, similar to those used by the two previous neutrino experiments. As will be shown below, the kinds of observations which can be obtained in each of the two methods are rather different.

1. Signals above Combinatorial Background

To estimate the distribution of combinatorial background in $\pi^+\pi^-$ invariant mass plots, mass combinations $(\pi_i^+\pi_j^-)$ were formed using different events, that is, (event i) $\neq$ (event j). In order to approximate energy conservation, the pairing of unassociated pions was performed separately for each charge multiplicity, between events having similar hadronic masses: $|W_i - W_j| < 500$ MeV. The background shape is then normalized to the data over a high-mass, "non-resonant" interval, for which 0.92 to 1.52 GeV was used. Because of the limited statistics of our event sample, this procedure with its resultant background could only be carried through in charge multiplicities ranging from four through seven prongs. However, a qualitative picture of resonance contributions to $(\pi^+\pi^-)$ mass correlations can be extracted, as shown in Figs. 3, 4, and 5: Fig. 3 shows the inclusive $(\pi^+\pi^+)$ mass distribution for four through seven prong events. The corresponding combinatorial background is given by the dashed curve, which should supposedly be a good representation of the data over all invariant masses since $\pi^+\pi^+$ is non-resonant. This is roughly the case, although at low masses the background tends to fall typically ten combinations per mass bin lower than the real data. This shortcoming is likely the result of our inability to associate pion pairs from different events in a more differential way and should improve with larger event samples. The inclusive $\pi^+\pi^-$ mass distribution for four through seven prong events is displayed in Fig. 4, together with the combinatorial background estimate (dashed curve). An excess above background in the ρ° region - 700 through 800 MeV/c^2 - is clearly seen.

If the combinatorial background in four through seven prong events is subtracted from the distribution of $(\pi^+\pi^-)$ invariant masses as shown in Fig. 5, two enhanced regions are observed. The peak at higher mass, which is centered around 750 MeV in $m(\pi^+\pi^-)$, we ascribe to ρ° decays; the broad excess above the combinatorial background appearing below the ρ° ($m(\pi^+\pi^-) \lesssim 600$ MeV) suggests abundant ω° and η° production, wherein only the charged pions are detected from 3-body decays $\pi^+\pi^-\pi^\circ$ and $\pi^+\pi^-\gamma$. In order to verify this interpretation improved γ detection efficiency for deuterium or hydrogen exposures would be required, as possibly afforded by a 10-20% mole $Ne \cdot H_2$ mixture or by a downstream plate array.(11) From Fig. 5 we conclude that ρ° production occurs in our data and that the signal can be isolated, provided that care is taken to minimize signal feed-in from the broad enhancement at lower mass.

2. Fit Using ρ° Breit-Wigner with Quadratic Background

To determine amounts of inclusive ρ° production contributed by all charge multiplicities, we fit the $\pi^+\pi^-$ mass spectrum in the interval $0.52 \leq m(\pi^+\pi^-) \leq 1.2$ GeV/c^2 using an incoherent sum of a P-wave Breit-Wigner amplitude-squared for the ρ° together with a quadratic background:

$$\frac{d\sigma}{dm} = F_{BG}(m)\ [\ a + b \cdot F_{BW}(m)] \tag{4}$$

where

$$F_{BG} = C_1 + C_2 m + C_3 m^2$$

and

$$F_{BW} = \frac{m \cdot m_R\ \Gamma(m)}{(m^2 - m_R^2) + m_R^2 \cdot \Gamma^2_{(m)}}$$

with

$$\Gamma(m) = \Gamma_R \cdot (q/q_R)^{2\ell+1} \cdot \frac{\rho(m)}{\rho(m_R)} ,$$

$$\rho(m) = (q_R^2 + q^2)^{-1}.$$

In the above expressions, m_R is the resonance mass, Γ_R is its width, q is the momentum of one of the decay products in the resonance rest frame, q_R is the q value at $m = m_R$; and a, b, c_1, c_2 and c_3 are parameters to be determined. This method has been used previously to determine resonance production in hadron-hadron collisions;[9] it is also the one used to measure ρ° production in $\bar{\nu}p$ collisions by the ANL-CMU-Purdue Collaboration[7]. Based upon the ρ° signal observed in four-through-seven prongs (Fig. 5), and also the behavior of preliminary fits to the data in which m_R and Γ_R were allowed to vary, all results presented here have been extracted using fits with the ρ° mass and width fixed at 0.755 GeV/c^2 and 0.155 GeV/c^2 respectively.

The inclusive $\pi^+\pi^-$ mass distribution for all events, together with the five-parameter fit (dashed curves) is shown in Fig. 6. The fit finds a total of 683 $\pm$ 157 $\rho^\circ \to \pi^+\pi^-$ combinations, with χ^2 per degree of freedom of 0.8. This amount corresponds to

$$(\rho^\circ/\text{event})_{\nu D \to CC} = 0.19 \pm 0.04$$

and

$$(\rho^\circ/\pi^+)_{\nu D} = 0.07 \pm 0.02$$

for neutrino scattering on deuteron (isoscalar) targets. The same fitting procedure was also used for neutron traget and proton target events separately[12]; for neutron target events we find

$$(\rho^\circ/\text{event})_{\nu n} = 0.18 \pm 0.06,$$

and for proton targets

$$(\rho^\circ/\text{event})_{\nu p} = 0.21 \pm 0.08.$$

As summarized in Table I, no significant target dependence is observed among overall inclusive ρ° production rates. In subsequent analyses we treat deuteron targets only, in order to maximize statistics.

In the $\nu_\mu p$ experiment(8), ρ° production was reported to be prominent in 5-prong events. In our data, ρ° production as a function of charge multiplicity is summarized in Table II, which lists production rates for 4-5 prong events, 6-7 prong events, and $\geq$ 8 prong events. The ratio ρ°/event is found to increase with increasing multiplicity; a similar but milder trend is observed for the ratio ρ°/π^+.

3. Comparison with $\bar{\nu}p$ Results

Our sample of deuteron target events is sufficiently large to enable separation into course bins for any given variable. Events within each bin can then be fitted to the Breit-Wigner plus polynomial background, expression (4), so that differential rates of form (3) can be extracted. In the following we present relative rates determined differentially for νD reactions and compare them with published results from the $\bar{\nu}p$ experiment,(7) in which a similar analysis was performed.

In ρ° production from $\bar{\nu}p$ charged current reactions, it has been suggested that two contributions are present; one component is central ($Y_R \simeq 0$), and the other is a current fragmentation process. Fig. 7 gives the CM rapidity distribution for ρ°'s observed in the $\bar{\nu}p$ data and in this experiment. In both experiments produced ρ°'s occur almost entirely within the range

$-1.0 < Y_R < 1.0$. In the νD reactions of this experiment, the ratio $\rho°$/event increases gradually with increasing rapidity; 67% of $\rho°$'s from νD collisions have $Y_R > 0.0$. However, no evidence for a sudden increase in $\rho°$ production in the forward CM is seen.

If we assume that the central contribution is symmetric about $Y_R = 0$ as was done in the $\bar{\nu}p$ analysis, then we estimate ~41% of produced $\rho°$'s result from current fragmentation processes, whereas at least 50% is indicated for $\bar{\nu}p$ reactions.

Measurements of W, Q^2, and p_T dependence of $\rho°$ production are summarized in Fig. 8 and Table III. As shown in Fig. 8(a), the ratio $\rho°$/event increases gradually throughout the accessible range of masses W of the hadronic system, for both νD and $\bar{\nu}p$ interactions. For p_T, the momentum of the $\rho°$ transverse to the hadronic system's longitudinal axis, the ratios ($\rho°$/event) and $(\rho°/\pi^{\pm})_{\nu,\bar{\nu}}$ are nearly identical in the two experiments and exhibit little p_T-dependence (Fig. 8(c)). The dependence of $\rho°$ production on Q^2, the four-momentum-transfer-squared to the hadronic system, is displayed in Fig. 8(b). In the $\bar{\nu}p$ data, for which $\langle Q^2 \rangle_{\bar{\nu}p}$ = 2.7 $(\text{GeV/c})^2$, no significant Q^2-dependence for inclusive $\rho°$ production is observed. However, in the νD reactions of this experiment, higher Q^2-transfer to the hadronic system is achieved, e.g. $\langle Q^2 \rangle = 14.06\ (\text{GeV/c})^2$. It is seen that although the νD data are completely consistent with the $\bar{\nu}p$ results in the lower Q^2-regime and are indeed everywhere compatible with no Q^2-dependence, nevertheless the highest Q^2 bins suggest a mild increase in $\rho°$ production with increasing Q^2.

V. CONCLUSIONS

In high energy neutrino-deuterium charged current interactions, we find:

1) Inclusively produced $K^{*+}(890)$ resonances occur nearly entirely as current fragments, with $K^{*+}(890)$/event = 0.05 ± 0.01 and $K^{*+}(890)/K^{\circ}_{s}$ = 0.23 ± 0.03.

2) Two broad enhancements in $\pi^{+}\pi^{-}$ invariant mass are observed above combinatorial background in 4-through-7 prongs. The higher mass enhancement is readily identified with ρ° decays; the broad, lower mass excess may reflect abundant ω° and η° production.

3) From deuteron target events, inclusive ρ° production occurs with the relative rates ρ°/event = 0.19 ± 0.04 and $\rho^{\circ}/\pi^{+} = 0.07 \pm 0.02$. Similar rates are found for neutron and proton target events separately.

4) The ratio ρ°/event is observed to increase with increasing charge multiplicity.

5) No evidence is found for a large current fragmentation component to inclusive ρ° production in νD reactions.

6) Relative rates ρ°/event and $(\rho^{\circ}/\pi^{+})_{\nu,\bar{\nu}}$ as functions of W, Q^2, and p_T are in agreement with results from $\bar{\nu}p$ interactions. However, in the higher Q^2 values probed by this experiment, a gradual increase in ρ°/event with increasing Q^2 is indicated.

We wish to acknowledge the staff of the Neutrino Laboratory at Fermilab for their excellent work during the experimental run. We also wish to thank the scanners and measurers at our collaborating institutions for their diligent efforts. This research is supported in part by the U.S. Department of Energy and the National Science Foundation.

FOOTNOTES AND REFERENCES

1. V. Blobel et al., Phys. Lett. 48B, 72 (1974).
2. H. Kirk et al., Nucl. Phys. B128, 397 (1977).
3. R. Raja et al., Phys. Rev. D16, 2733 (1977).
4. R. Singer et al., Phys. Lett. 60B, 385 (1976).
5. H. Kichimi et al., Phys. Rev. D20, 37 (1979).
6. R. Diebold, in: Proceedings of the 19th International Conference on High Energy Physics, Tokyo, Aug. 23-30, 1978; p.666.
7. M. Derrick et al., Phys. Lett. 91B, 307 (1980).
8. J.P. Berge et al., Preprint UH-511-368-79, to be published in Physical Review, 1980.
9. J. Canter et al., Phys. Rev. D20, 1029 (1979).
10. N. Schmitz, in: Proceedings of the 1979 International Symposium on Lepton and Photon Interactions at High Energies, Fermilab, Aug. 23-29, 1979; p.359.
11. J. Hanlon, W.A. Mann, S. Sommars, H. Wald, in: Proceedings of the Topical Conference on Neutrino Physics, Oxford, July, 1978.

12. To first approximation, ignoring rescattering, neutron-target events can be identified with even charge multiplicities and proton target events with odd multiplicities provided that visible spectator protons ($<$ 20% of neutron target events) are not included in the charged prong count. However, protons with production angles in the LAB forward with respect to the beam may possibly be other than spectators. Hence, only production angles which are backward are tagged as spectators; corresponding numbers of forward spectator proton events are accounted for by event

weighting. In addition, the effects of final state rescattering within the deuteron, which enhances proton target samples at the expense of neutron target samples, are corrected for using event weights. For details, see J. Hanlon et al., in: Proceedings of the International Conference NEUTRINO '79, Bergen, Norway, 18-22 June, 1979.

TABLE I

Relative Rates for Inclusive ρ° Production in

ν D Charged Current Events

	ρ°/ C.C. Event	ρ°/π^+	ρ°/π^-
Deuteron	0.19 ± 0.04	0.07 ± 0.02	0.15 ± 0.04
Neutron	0.18 ± 0.06	0.08 ± 0.03	0.14 ± 0.05
Proton	0.21 ± 0.08	0.07 ± 0.03	0.17 ± 0.07

TABLE II

Relative Rates for ρ° Production Versus Charge Multiplicity

	ρ°/CC Event	ρ°/π^+	ρ°/π^-
4–5 prong	0.11 ± 0.01	0.04 ± 0.01	0.15 ± 0.01
6–7 prong	0.38 ± 0.06	0.11 ± 0.02	0.24 ± 0.04
$\geq$ 8 prong	0.61 ± 0.23	0.13 ± 0.05	0.22 ± 0.09

TABLE III

Differential Rates for ρ° Production

ρ° Production Versus Y_R

	$Y_R < -0.5$	$-0.5 < Y_R < 0.0$	$0.0 < Y_R < 0.5$	$Y_R > 0.5$
ρ°/event	0.02 ± 0.02	0.04 ± 0.01	0.06 ± 0.02	$0.07 {}^{+0.03}_{-0.02}$
ρ°/π^+	0.03 ± 0.02	0.09 ± 0.02	0.12 ± 0.04	$0.07 {}^{+0.02}_{-0.02}$

ρ° Production Versus W

	W < 3.0 GeV	3.0 < W < 4.8 GeV	W > 4.8 GeV
ρ°/event	$0.08 {}^{+0.05}_{-0.04}$	0.13 ± 0.06	0.31 ± 0.06
ρ°/π^+	$0.04 {}^{+0.03}_{-0.02}$	0.05 ± 0.02	0.10 ± 0.02

ρ° Production Versus Q^2

	$Q^2 < 2.5$ GeV	$2.5 < Q^2 < 5.0$ GeV	$5.0 < Q^2 < 10.0$ GeV	$Q^2 > 10.0$ GeV
ρ°/event	0.10 ± 0.06	0.10 ± 0.06	$0.23 \pm .010$	0.32 ± 0.10
ρ°/π^+	0.05 ± 0.03	0.04 ± 0.02	0.08 ± 0.04	0.10 ± 0.03

ρ° Production Versus p_T

	$p_T < 2.5$ GeV	$2.5 < p_T < 5.0$ GeV	$p_T > 5.0$ GeV
ρ°/event	0.06 ± 0.01	0.06 ± 0.01	0.07 ± 0.02
ρ°/π^+	0.05 ± 0.01	0.06 ± 0.01	0.13 ± 0.03

FIGURE CAPTIONS

Fig. 1. The invariant mass distribution $m(K^\circ_s\pi^\pm)$ from inclusive reactions $\nu_\mu + D \to \mu^- + (K^\circ_s\pi^\pm) + X$. The combinations $K^\circ_s\pi^+$ are shown shaded. The dotted and cross-ed distributions show the combinatorial backgrounds (see text) normalized to the histogrammed areas.

Fig. 2. The invariant mass distribution $m(K^\circ_s\pi^+)$. (a) Combinations produced forward ($Y_R > 0.0$) and backward ($Y_R < 0.0$) in the hadronic system's center-of-mass.

Fig. 3. Invariant mass distribution for $\pi^+\pi^+$ pairs from multiplicities 4 through 7 prongs. The dot-dashed curve shows the uncorrelated background distribution obtained by associating pions from different events but having the same multiplicity and hadronic mass. The background curve is normalized to the data over the mass interval 0.92 to 1.52 GeV.

Fig. 4. Invariant mass distribution for $\pi^+\pi^-$ pairs from multiplicities 4 through 7 prongs. The superimposed curve shows the estimated distribution of uncorrelated background (see text).

Fig. 5. Correlated $\pi^+\pi^-$ invariant mass obtained by subtracting the distributions of Fig. 4.

Fig. 6. Invariant mass of $\pi^+\pi^-$ pairs from all multiplicities, with fit using incoherent sum of quadratic background plus p-wave Breit-Wigner form shown superimposed.

Fig. 7. Inclusive production ratios ρ°/event (open triangles) and $\rho^\circ/\pi^\pm|_{\nu,\bar{\nu}}$ (open circles) versus Y_R, the center-of-mass rapidity in the hadron system, (a) for $\bar{\nu}p$ reactions (ANL-CML-Purdue) and (b) for νD reactions (this experiment).

Fig. 8. Comparison of production ratios ρ°/event in $\bar{\nu}p$ data (open triangles) and νD data of this experiment (closed diamonds), versus mass of the hadronic system W, four-momentum transfer to the hadronic system Q^2, and momentum transverse to the hadronic jet axis p_T.

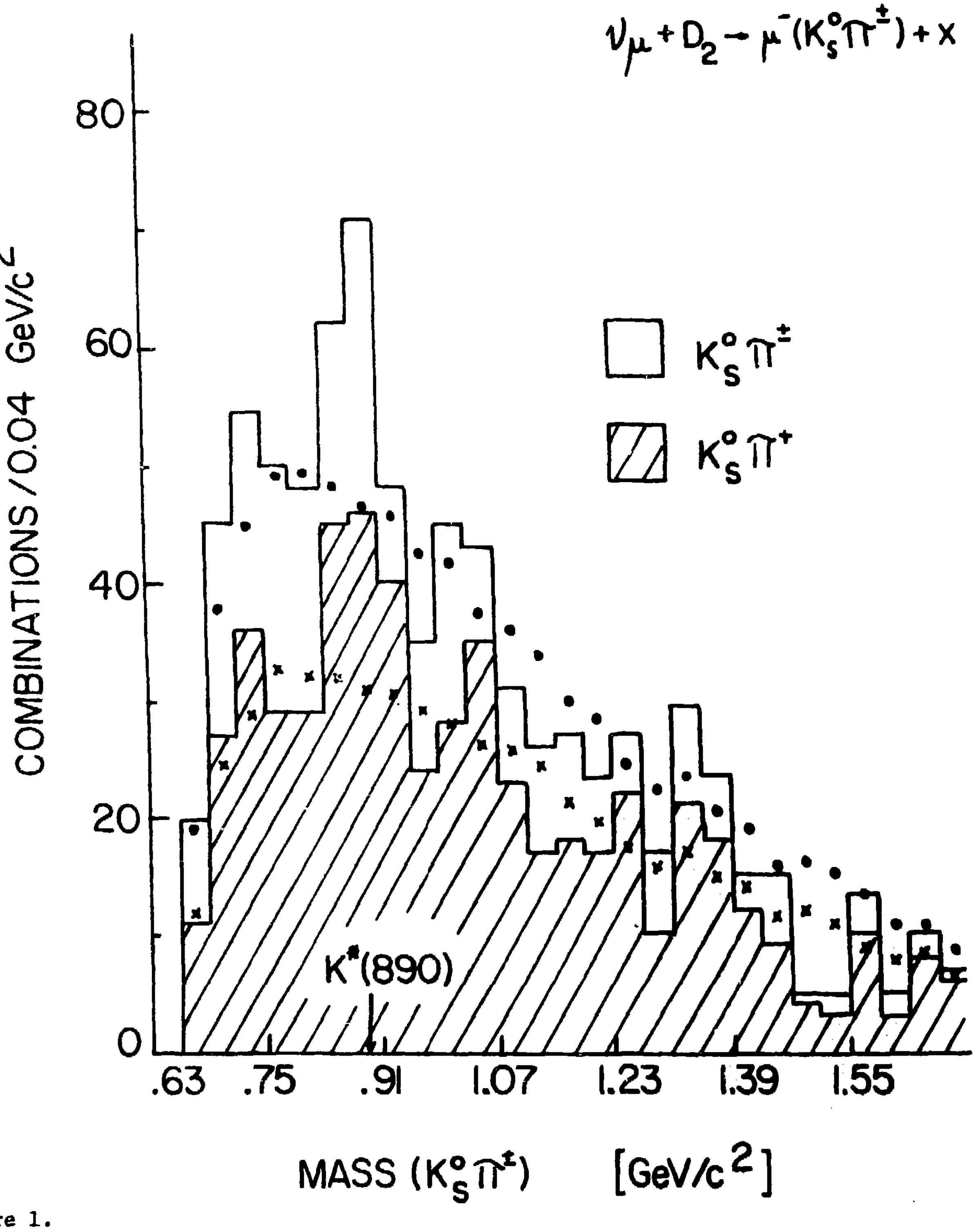
$\nu_\mu + D_2 \rightarrow \mu^- (K^o_s \pi^\pm) + X$
80
60
40
20
0
COMBINATIONS/0.04 GeV/c²
$K^o_s \pi^\pm$
$K^o_s \pi^+$
K*(890)
.63
.75
.91
1.07
1.23
1.39
1.55
MASS ($K^o_s \pi^\pm$) [GeV/c²]

Figure 1.

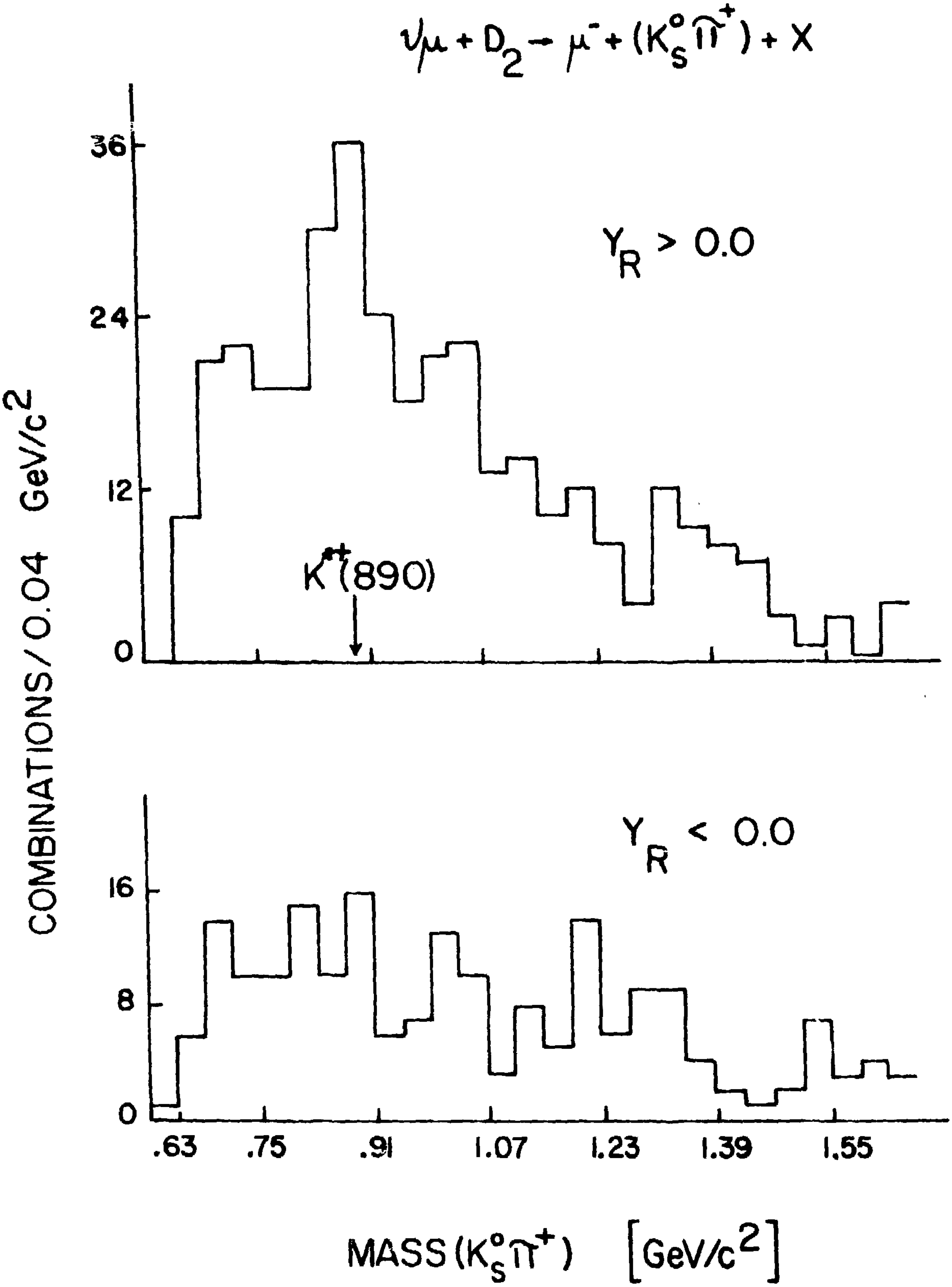

$\nu_\mu + D_2 \to \mu^- + (K^o_s \pi^+) + X$
36
24
12
0
$Y_R > 0.0$
$K^{*+}(890)$
COMBINATIONS/0.04 GeV/c^2
16
8
0
$Y_R < 0.0$
.63
.75
.91
1.07
1.23
1.39
1.55
MASS $(K^o_s \pi^+)$ [GeV/c^2]

Figure 2 (a), 2 (b).

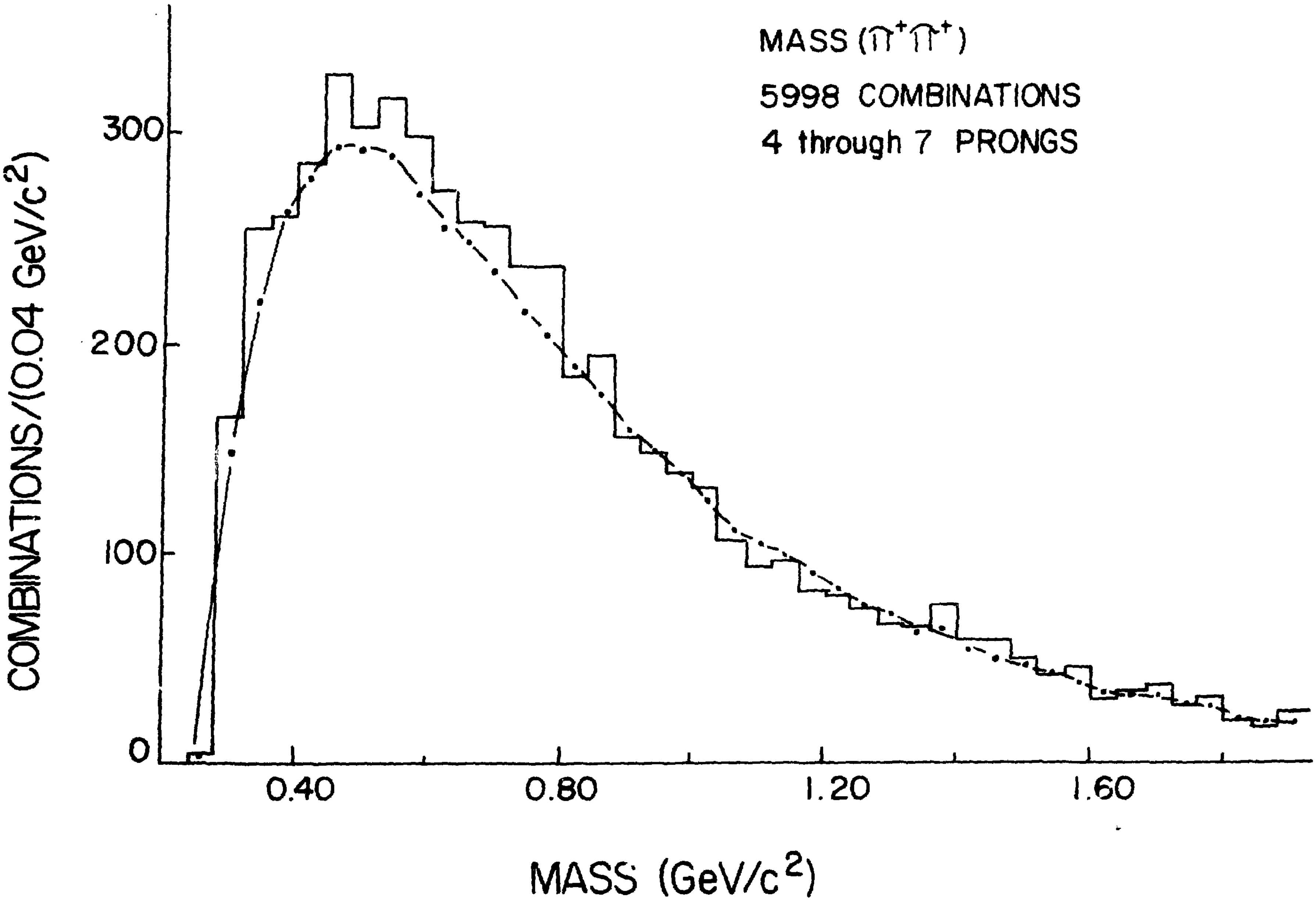
MASS (π⁺π⁺)
5998 COMBINATIONS
4 through 7 PRONGS
COMBINATIONS/(0.04 GeV/c²)
300
200
100
0
0.40
0.80
1.20
1.60
MASS (GeV/c²)

Figure 3.

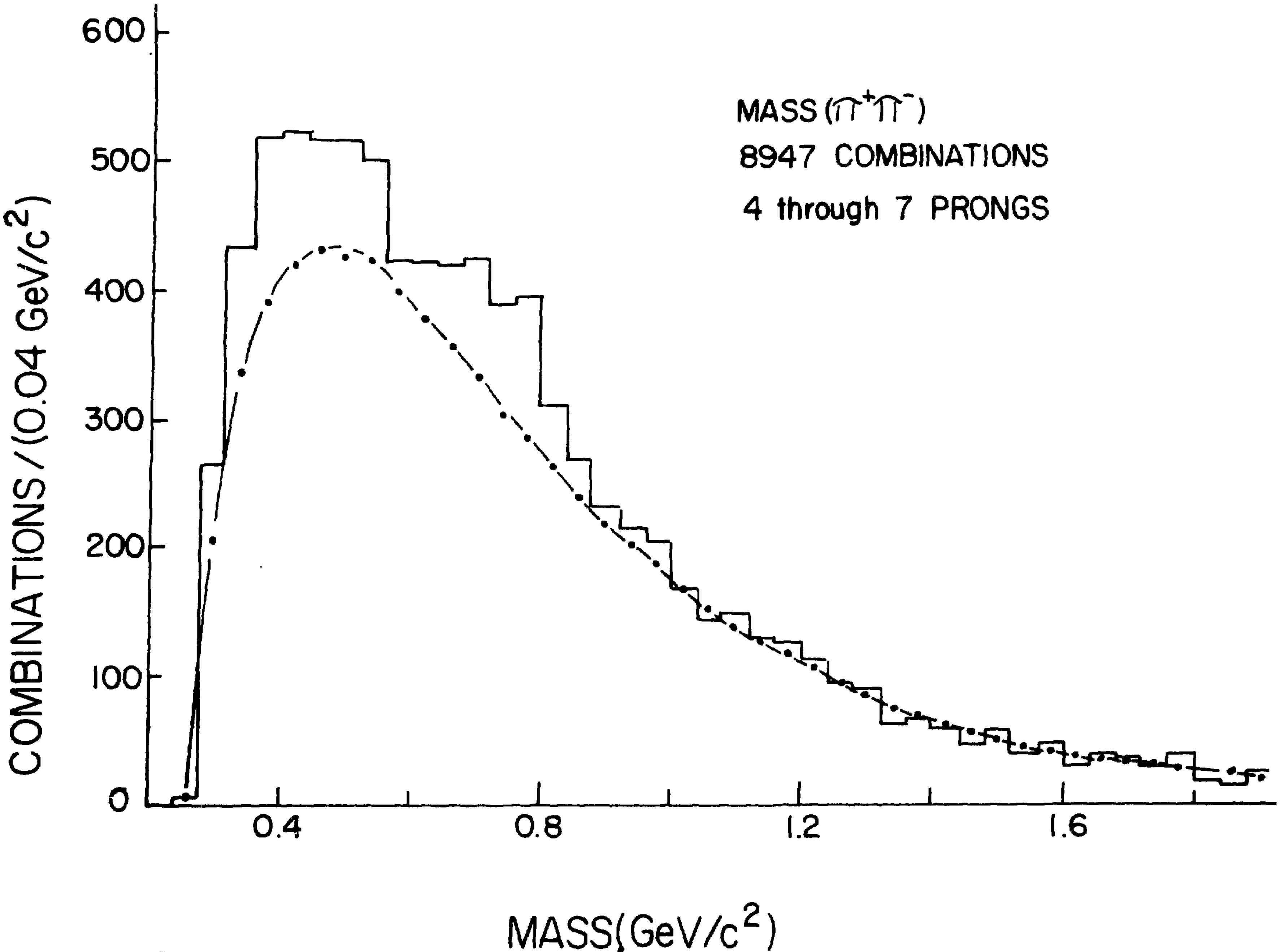

MASS ($\pi^+\pi^-$)
8947 COMBINATIONS
4 through 7 PRONGS
600
500
400
300
200
100
0
COMBINATIONS / (0.04 GeV/c^2)
0.4
0.8
1.2
1.6
MASS (GeV/c^2)

Figure 4.

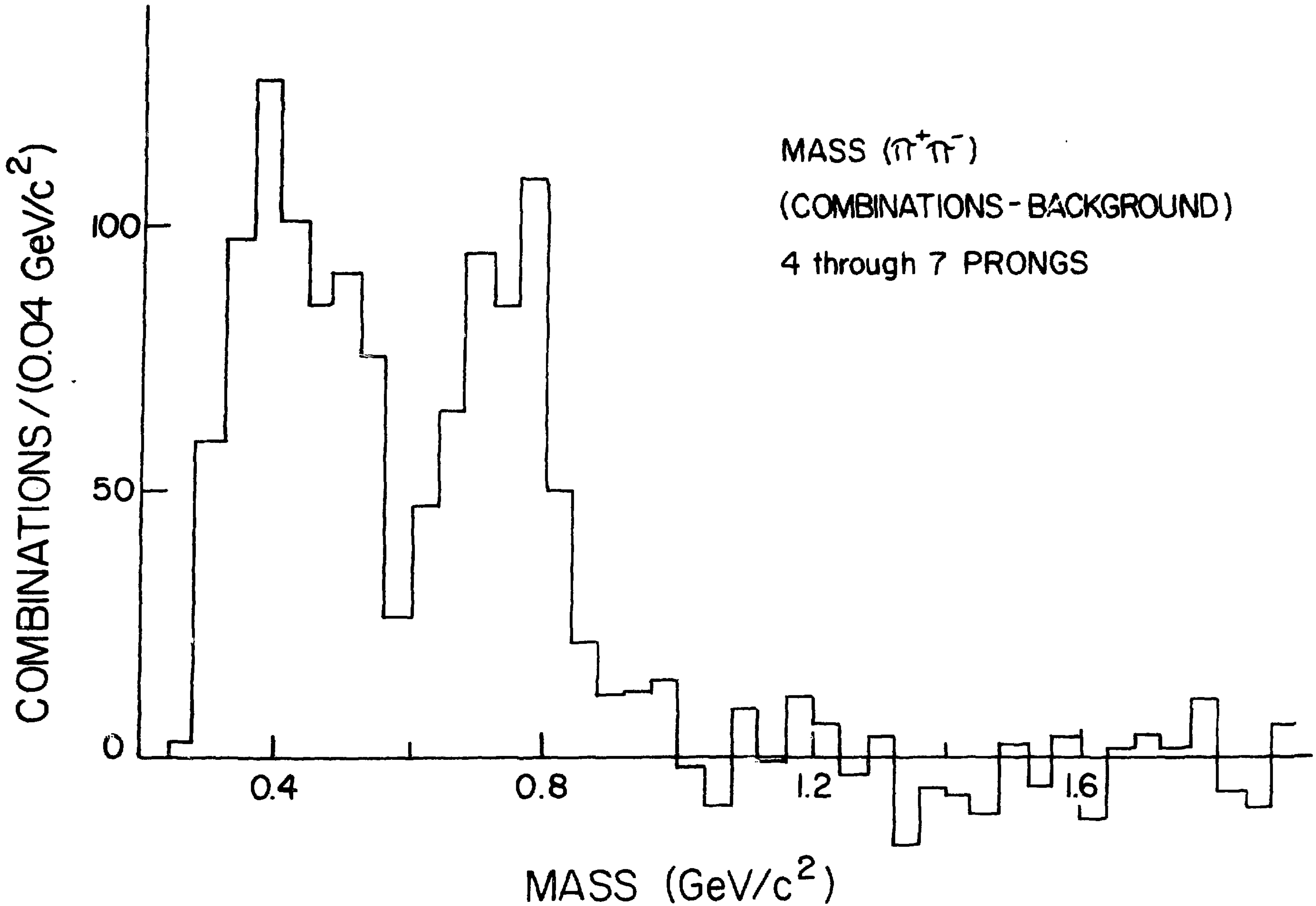
MASS ($\pi^+\pi^-$)
(COMBINATIONS - BACKGROUND)
4 through 7 PRONGS
COMBINATIONS / (0.04 GeV/c^2)
100
50
0
0.4
0.8
1.2
1.6
MASS (GeV/c^2)

Figure 5.

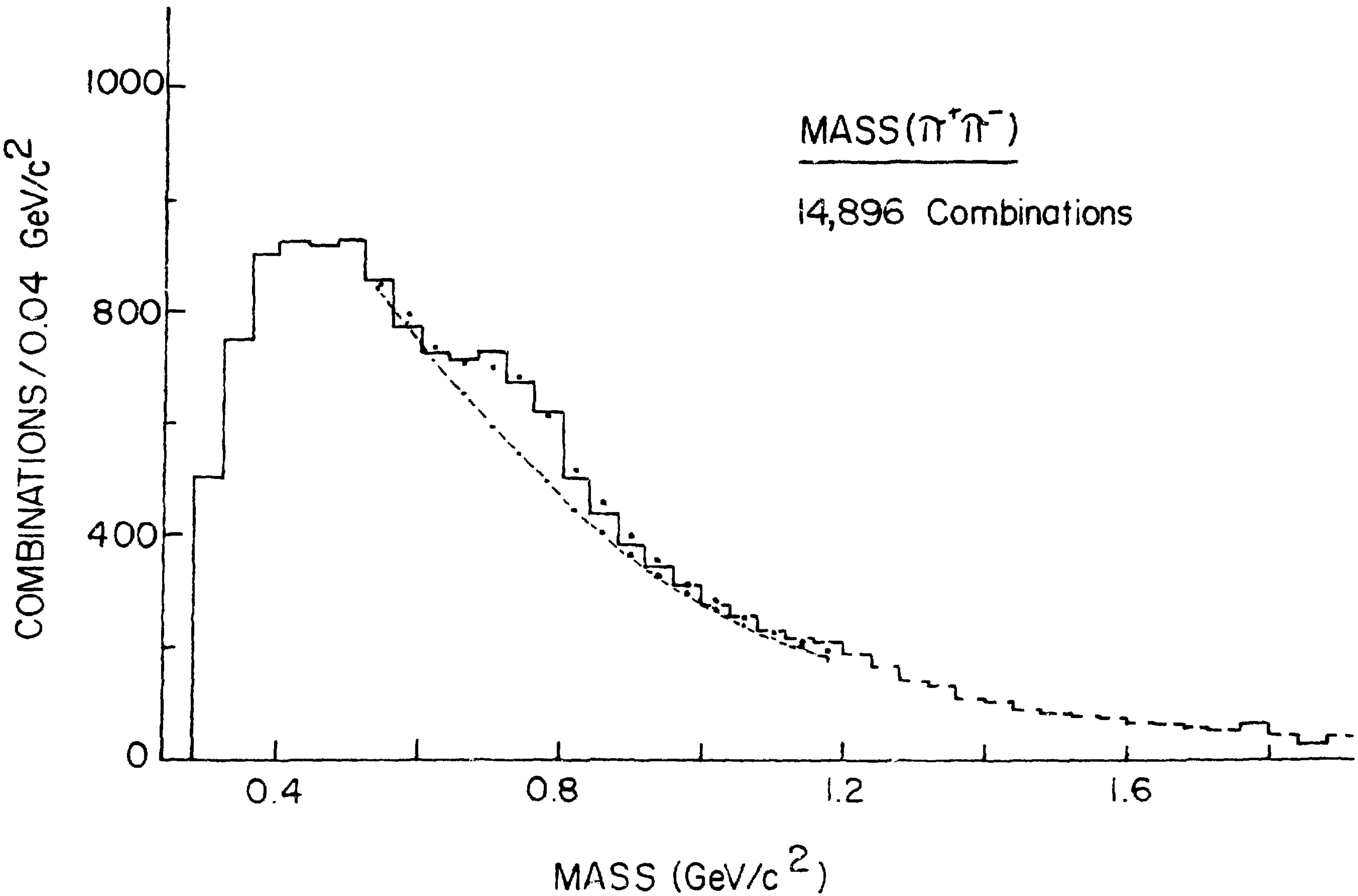

MASS($\pi^+\pi^-$)
14,896 Combinations
COMBINATIONS/0.04 GeV/c^2
1000
800
400
0
0.4
0.8
1.2
1.6
MASS (GeV/c^2)

Figure 6.

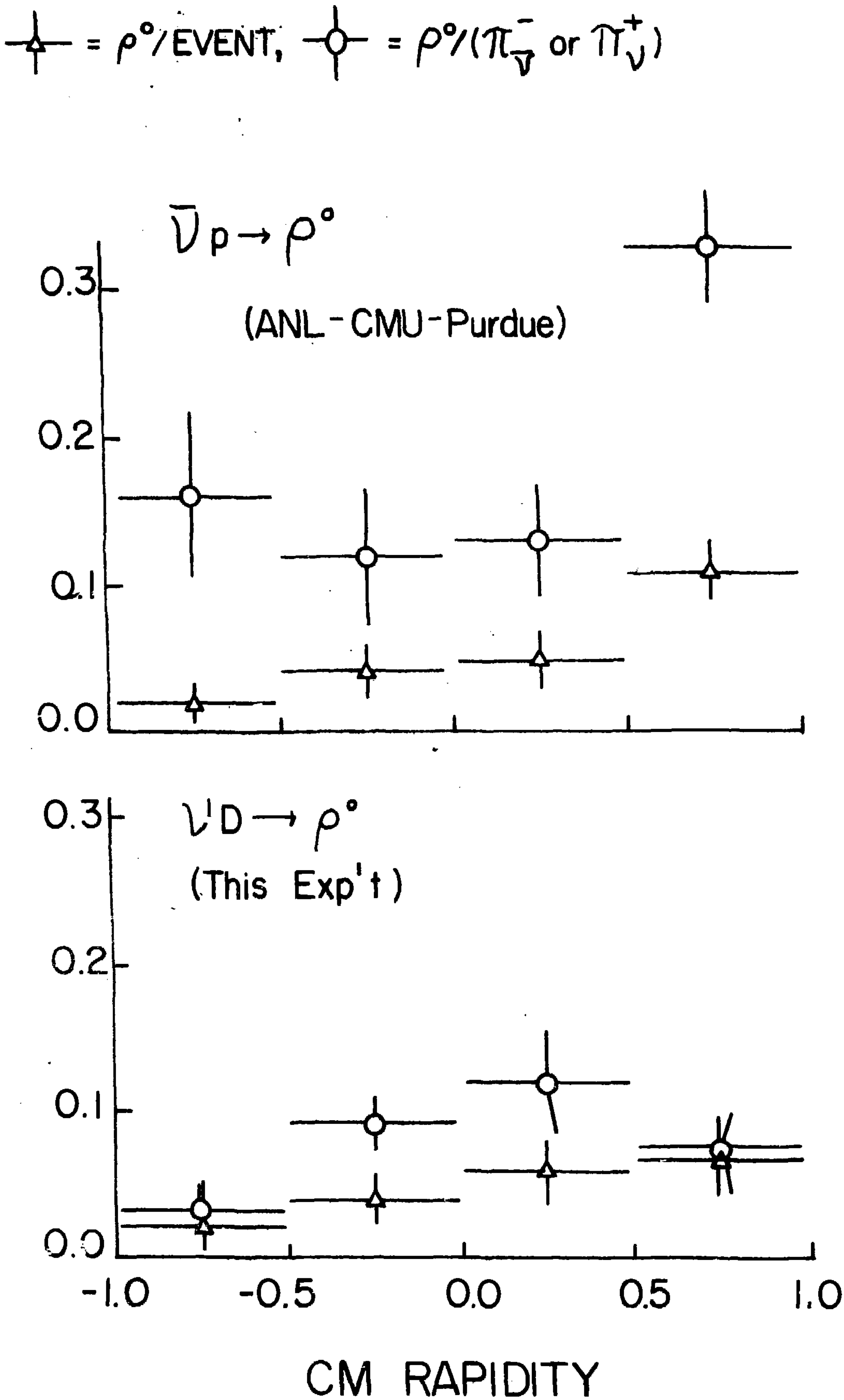
= ρ°/EVENT, = ρ°/(π⁻ν̄ or π⁺ν)
ν̄p → ρ°
(ANL-CMU-Purdue)
0.3
0.2
0.1
0.0
νD → ρ°
(This Exp't)
0.3
0.2
0.1
0.0
-1.0
-0.5
0.0
0.5
1.0
CM RAPIDITY

Figure 7 (a), 7 (b).

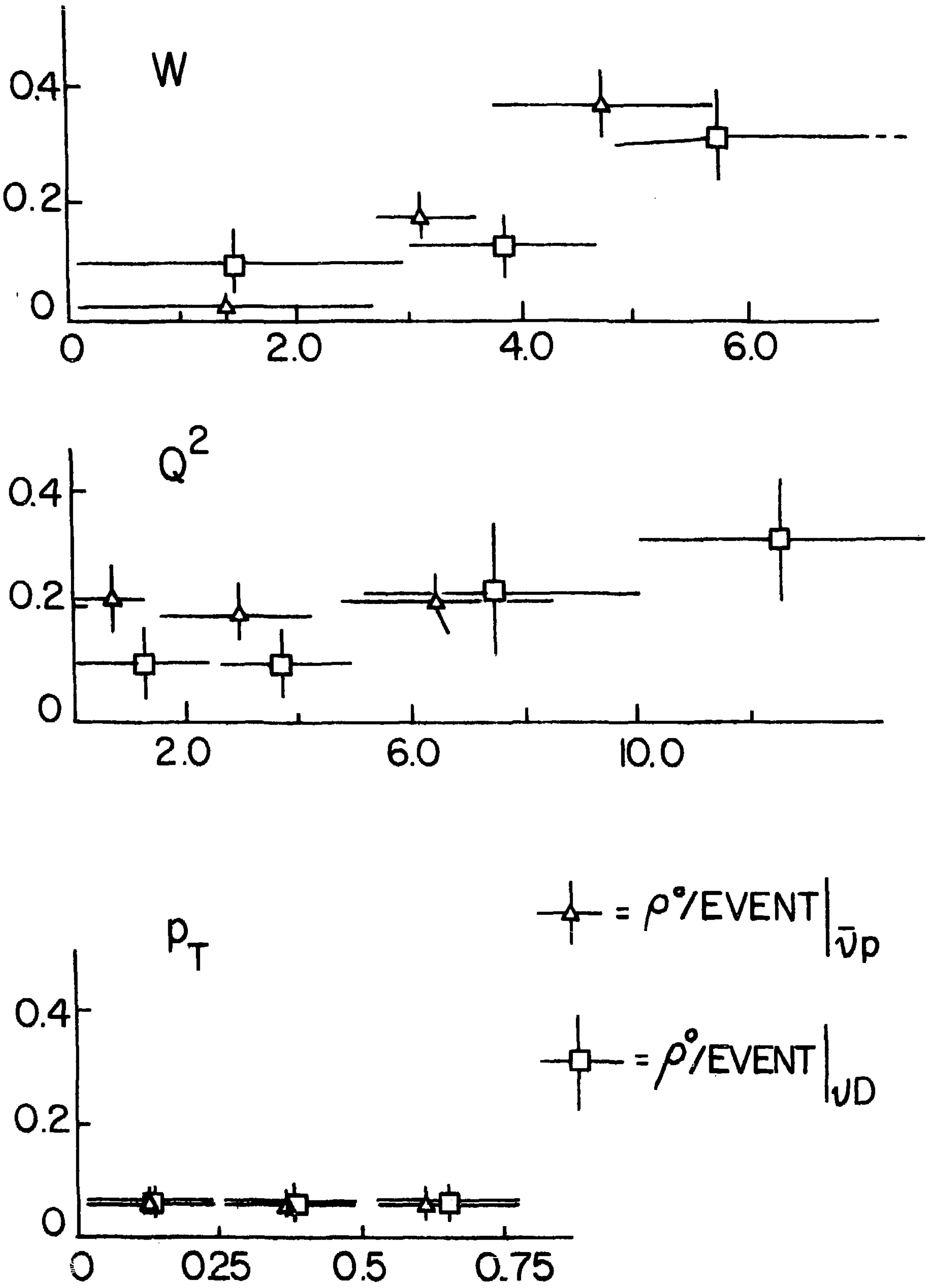

Figure 8 (a), 8 (b), 8 (c).